

# Aqueous synthesis of CdTe@FeOOH and CdTe@Ni(OH)<sub>2</sub> composited nanoparticles

Liang Li, Jicun Ren\*

College of Chemistry & Chemical Engineering, Shanghai Jiaotong University, 800 Dongchuan Road, Shanghai 200240, PR China

Received 16 November 2005; received in revised form 20 March 2006; accepted 20 March 2006

Available online 27 March 2006

## Abstracts

Two kinds of bi-functional nanomaterials, CdTe@FeOOH and CdTe@Ni(OH)<sub>2</sub>, were synthesized in water phase. In the synthesis, using the luminescent CdTe nanocrystals (NCs) as a core, Fe<sup>3+</sup> (Ni<sup>2+</sup>) was added to CdTe NCs aqueous solution and slowly hydrolyzed to deposit a layer of hydroxide onto the luminescent CdTe NCs in the presence of stabilizer. TEM, XRD, XPS, UV, fluorescence spectrometer and physical property measurement system (PPMS) were used to characterize the final products, and the results showed that the as-prepared nanoparticles with core/shell structure exhibited certain magnetic properties and fluorescence.

© 2006 Elsevier Inc. All rights reserved.

**Keywords:** Fluorescence; Magnetic; Nanoparticle; Bi-functional; CdTe; FeOOH; Ni(OH)<sub>2</sub>

## 1. Introduction

Integrating different materials with unique properties into one entity have attracted much attention because of their potential applications [1–9]. Recently, several synthetic protocols for magnetic/luminescent bi-functional nanomaterials have been reported [3–9]. Encapsulating into silica nanoparticles [8], dumbbell [6,9], and core/shell structures [4,5,7] were the usual architectural strategies to combine two kinds of materials with specific functions. We found the most successful reports about bi-functional nanomaterials were usually prepared by organometallic chemistry. Rare reports on the synthesis of bi-functional nanomaterials in aqueous solution have been appeared. Recently, we put forward a new protocol for preparing fluorescent and magnetic bi-functional nanoparticles in water phase [10]. We used the fluorescent nanocrystals (NCs) prepared in aqueous solution as seeds, and then deposited magnetic materials on them to obtain two functions in a material. As is known, the Ni and Fe hydroxides have some important properties such as electrochemical activity, magnetism and catalysis. In this

paper, Fe<sup>3+</sup> or Ni<sup>2+</sup> were added into CdTe NCs aqueous solution, which was hydrolyzed into FeOOH and Ni(OH)<sub>2</sub> and deposited onto CdTe NCs. Interestingly, the resulted nanoparticles with a shell of metal hydroxides still kept good optical properties, and the magnetic characterization results indicated that the two kinds of nanomaterials possessed certain magnetic behaviors. These products have some potential applications, such as magnetic resonance (MR)/optical imaging, being used as catalyst and magnetic–optical materials.

## 2. Experimental section

### 2.1. Materials

3-Mercaptopropionic acid (MPA, 99 + %) was product of Fluka, and rhodamine 6G (95%) was from Sigma-Aldrich. CdCl<sub>2</sub>·2H<sub>2</sub>O (99%), NaBH<sub>4</sub> (96%), and tellurium powder (99.999%, about 200 mesh), Ni(NO<sub>3</sub>)<sub>2</sub>·2H<sub>2</sub>O, FeCl<sub>3</sub>·6H<sub>2</sub>O (analytical grade) were obtained from Shanghai Reagent Company. The ultrapure water with 18.2 MΩ (Millipore Simplicity, USA) was used in all synthesis.

\*Corresponding author. Fax: +86 21 54741297.

E-mail address: [Jicunren@sjtu.edu.cn](mailto:Jicunren@sjtu.edu.cn) (J. Ren).

## 2.2. Preparation of composite nanoparticles

Firstly, the highly luminescent CdTe NCs were prepared according to the method reported previously [11,12]. The composite nanoparticles were prepared by the injection of  $\text{Fe}^{3+}$  ( $\text{Ni}^{2+}$ ) solutions into CdTe solutions and formed metal hydroxide shell on CdTe NCs. In a typical synthesis, 2 mL of 0.01 M  $\text{FeCl}_3$  aqueous solutions was added into 100 mL 1 mM CdTe colloid solution (MPA, 2 mM), and then adjusted to pH 11 with 1 M NaOH. The solution was placed in a three-necked flask and was heated to 96 °C with condenser attached to reflux for a set time. In the presence of MPA and weak basic solution,  $\text{Fe}^{3+}$  ( $\text{Ni}^{2+}$ ) hydrolyzed and formed hydroxide to deposit on the surfaces of CdTe NCs. It should be noticed,  $\text{Fe}(\text{OH})_3$  gets easily converted to oxyhydroxide ( $\text{FeOOH}$ ) [13,14]. The adding and refluxing process can be repeated several times for coating more hydroxides on CdTe NCs.

## 2.3. Characterizations

UV-visible absorption spectra were measured with a Lambda 20 UV-visible spectrophotometer (Perkin/Elmer). Fluorescence experiments were performed with a Varian Cary spectrometer. Samples were prepared by diluting colloidal solutions with water. The quantum yield (QY) of CdTe NCs was measured (Rhodamine 6G was chosen as reference standard, QY 95%) according to the method described in Ref. [15]. All optical measurements were performed at room temperature under ambient conditions.

X-ray powder diffraction (XRD) patterns were taken by a BRUKER-AXS D8 X-ray diffractometer. Transmission electron microscopy (TEM) was performed by a JEM-100CX (accelerating voltage of 100 kV) in order to analyze the size and structure of the resulted samples. X-ray photoelectron spectroscopy (XPS) was investigated by a MICROLAB MK II spectrometer with an  $\text{MgK}\alpha$  excitation (1253.6 eV); binding energy calibration was based on  $\text{C}1s$  at 284.6 eV. The thermogravimetry-differential thermal analysis (TG-DTA) was conducted in the temperature range 25–800 °C at a rate of 20 °C/min under an  $\text{N}_2$  atmosphere. The isothermal field-dependent magnetizations were measured at room temperature in a Quantum Design physical property measurement system (PPMS, USA).

## 3. Results and discussion

Fig. 1 shows the absorption spectra and fluorescent spectra of CdTe NCs before and after coating the  $\text{FeOOH}$  or  $\text{Ni}(\text{OH})_2$  shell. With the injection of  $\text{Fe}^{3+}$  ( $\text{Ni}^{2+}$ ) solution and the further refluxing, the absorbance and emission of CdTe NCs shifts to longer wavelength. Typically, after three-times adding of  $\text{Fe}^{3+}$  solution and refluxing, the emission peak of the resulted composite nanoparticles ( $\text{B}_3$ ) shifted from 567 ( $\text{A}_0$ ) to 640 nm, and at the same time, decreased dramatically to 10% from the original 58%. Similar phenomena were also observed in the coating of  $\text{Ni}(\text{OH})_2$  on CdTe NCs, but the photoquenching effect was not so severe. The sample  $\text{C}_3$  still shows a QY of

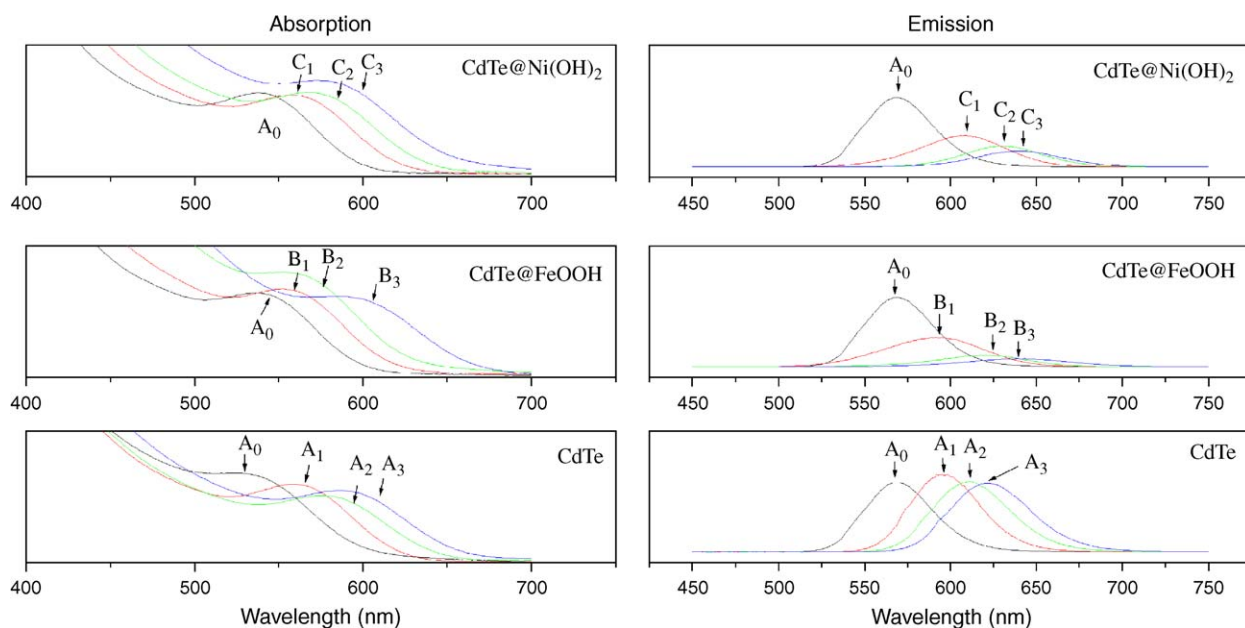


Fig. 1. The fluorescent spectra (right) and their corresponding absorption spectra (left) of MPA-coated CdTe, CdTe@FeOOH, CdTe@Ni(OH)<sub>2</sub> nanoparticles. ( $\text{A}_0$ : the crude CdTe solution;  $\text{A}_1$ : the sample taken after refluxing  $\text{A}_0$  for 1 h;  $\text{A}_2$ : the sample taken after refluxing  $\text{A}_0$  for 2 h;  $\text{A}_3$ : the sample taken after refluxing  $\text{A}_0$  for 3 h;  $\text{B}_1(\text{C}_1)$ : the sample taken after the first adding of  $2 \text{ mL} \times 10^{-2} \text{ M}$   $\text{Fe}^{3+}$  ( $\text{Ni}^{2+}$ ) solution to 100 mL crude CdTe solution and further refluxing for 1 h;  $\text{B}_2(\text{C}_2)$ : the sample taken after the second adding of  $2 \text{ mL} \times 10^{-2} \text{ M}$   $\text{Fe}^{3+}$  ( $\text{Ni}^{2+}$ ) solution into sample  $\text{B}_1(\text{C}_1)$  and further refluxing for 1 h;  $\text{B}_3(\text{C}_3)$ : the sample taken after adding  $2 \text{ mL} \times 10^{-2} \text{ M}$   $\text{Fe}^{3+}$  ( $\text{Ni}^{2+}$ ) solution into sample  $\text{B}_2(\text{C}_2)$  and further refluxing for 1 h.)

17%. The absorption and emission of the crude CdTe solution without adding metal cation also shifts longer wavelength with refluxing because of the growth of CdTe NCs, but the redshift is far less than that by adding  $\text{Fe}^{3+}$  ( $\text{Ni}^{2+}$ ). So the bigger redshift after the coating of the ferric oxyhydroxide or nickel hydroxide cannot only be owed to the growth of CdTe NCs. Furthermore, the redshift of emission was larger than that of absorption, which led to that the Stokes shift became larger (Fig. S1) with the adding  $\text{Fe}^{3+}$  ( $\text{Ni}^{2+}$ ) and refluxing. For the samples with similar emission spectra, the Stokes shifts of sample C<sub>3</sub> (emission at 640 nm), B<sub>3</sub> (emission at 640 nm), and A<sub>3</sub> (emission at 623 nm) were 67, 54 and 41 nm, respectively. The dramatic redshift, larger Stokes shift and photoquenching were possibly attributed to the coating of hydroxides or the doping of  $\text{Fe}^{3+}$  ( $\text{Ni}^{2+}$ ) into CdTe NCs by cation exchange on the surface of CdTe NCs.

As shown in Fig. 2, after the coating of metal hydroxides, the intensities of XRD pattern peak of the composite nanoparticles became weaker than that of the crude sample, and lightly shifts to larger angle. According to the recent work by Alivisatos et al. [16], cation exchange could happen at the interface of NCs and bulk solution, which could change the structure of NCs and further affect their optical properties. In our experiments,  $\text{Fe}^{3+}$  ( $\text{Ni}^{2+}$ ) could exchange  $\text{Cd}^{2+}$  from the surface of CdTe NCs and doping into CdTe NCs, and this probably was the main reason for the redshift of absorption/emission spectra and the changes in XRD patterns of the as-prepared composite nanoparticles.

The representative TEM images of CdTe seeds, CdTe@FeOOH and CdTe@Ni(OH)<sub>2</sub> composite nanoparticles are shown in Fig. 3. The sizes of CdTe NCs averaged about 3 nm, and the CdTe@FeOOH and CdTe@Ni(OH)<sub>2</sub> composite nanoparticles averaged 5 and 7 nm, respectively. It is very evident that the particles after coating hydroxides

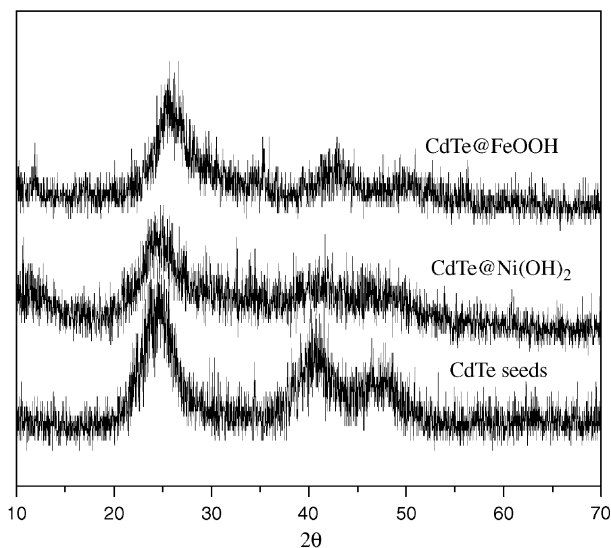


Fig. 2. The XRD patterns obtained from the CdTe@Ni(OH)<sub>2</sub> and CdTe@FeOOH powders and their corresponding CdTe seeds.

were bigger than the uncoated CdTe seeds, and the HRTEM images (Figs. 3E and F) of the resulted composite nanoparticles further confirmed the formation of the core/shell structure. The corresponding energy-dispersive X-ray spectrometry (EDX) results indicated the presence of Fe (Ni) in these nanoparticle as well as Cd, Te and S. The Cd and Te were from CdTe, Fe or Ni was from the coating shell, and the S was attributed to the stabilizer of MPA. Those all proved the successful coating of FeOOH or Ni(OH)<sub>2</sub> on CdTe NCs (Fig. 4).

Fig. 5 shows the typical TG-DTA curves of the CdTe NCs, CdTe@FeOOH nanoparticles and CdTe@Ni(OH)<sub>2</sub> nanoparticles measured under an N<sub>2</sub> atmosphere during heating. The thermogravimetric pattern of CdTe NCs exhibits two evident weight-loss steps; the first weight-loss step below 150 °C was due to removal of various types of water, and the latter above 400 °C possibly corresponds to the decomposition of Cd-MPA complexes. The thermal behaviors of CdTe@FeOOH and CdTe@Ni(OH)<sub>2</sub> were different from that of CdTe seeds, and their DTA curves (Figs. 5B and C) both have an additional endothermic peak between 200 and 400 °C, which must be from something that is not existed in CdTe seeds. It was found as regards FeOOH that there is an endothermic peak around 270 °C due to the crystal transition of FeOOH to Fe<sub>2</sub>O<sub>3</sub> [17,18], such a value is similar to the value in Fig. 5B. The thermal behavior of Ni(OH)<sub>2</sub> was also studied previously [19–21], and there is a characteristic endothermic peak around 270–280 °C due to the dehydration of Ni(OH)<sub>2</sub> and formation of NiO, which is closed to the peak at 270 °C in the DTA curve of Fig. 5C. Based on the above analysis and the chemistry of iron oxyhydroxides and nickel hydroxides, we concluded that the Fe element in the composite nanomaterials mainly existed as FeOOH and that the Ni mainly existed as Ni(OH)<sub>2</sub>. Such speculations were further proved by XPS characterizations.

The low-resolution XPS survey spectra (Figs. S4A and B) confirmed the EDX results, and all desired elements were observed in the resulted composite nanoparticles. In order to reveal the chemical states of Fe and Ni atoms, the high-resolution XPS spectra of Fe2*p* and Ni2*p* regions were recorded. As shown in Figs. 4A and B, the peaks at 723.8 and 710.5 eV in Fe2*p* spectra are the features of Fe3*p*<sub>1/2</sub> and Fe3*p*<sub>3/2</sub>, which are well within the acceptable range for Fe (III) complexes [22,23]. The peak of Fe2*p*<sub>3/2</sub> at 710.5 eV was further analyzed with deconvolution software, and found that Fe possibly remains in two environments (FeOOH, Fe<sub>2</sub>O<sub>3</sub>). The peak at 711.5 eV can be assigned to FeOOH because such a value is close to the value (711.9 ± 0.2 eV) in Ref. [23], and the peak at 709.8 eV shows the existence of Fe<sub>2</sub>O<sub>3</sub> in the shell of CdTe@FeOOH nanoparticles [22–24], which was from the dehydration of FeOOH. The Ni2*p* spectrum shows the characteristic spin-orbit splitting (Ni2*p*<sub>3/2</sub> and Ni2*p*<sub>1/2</sub>) of nickel ions at 855.9 and 861.1 eV. Those peaks have been usually assigned to Ni<sup>2+</sup> ions associated to oxygen and hydroxide [22]. As shown in Fig. 4B, the most intense Ni2*p*<sub>3/2</sub> peak at

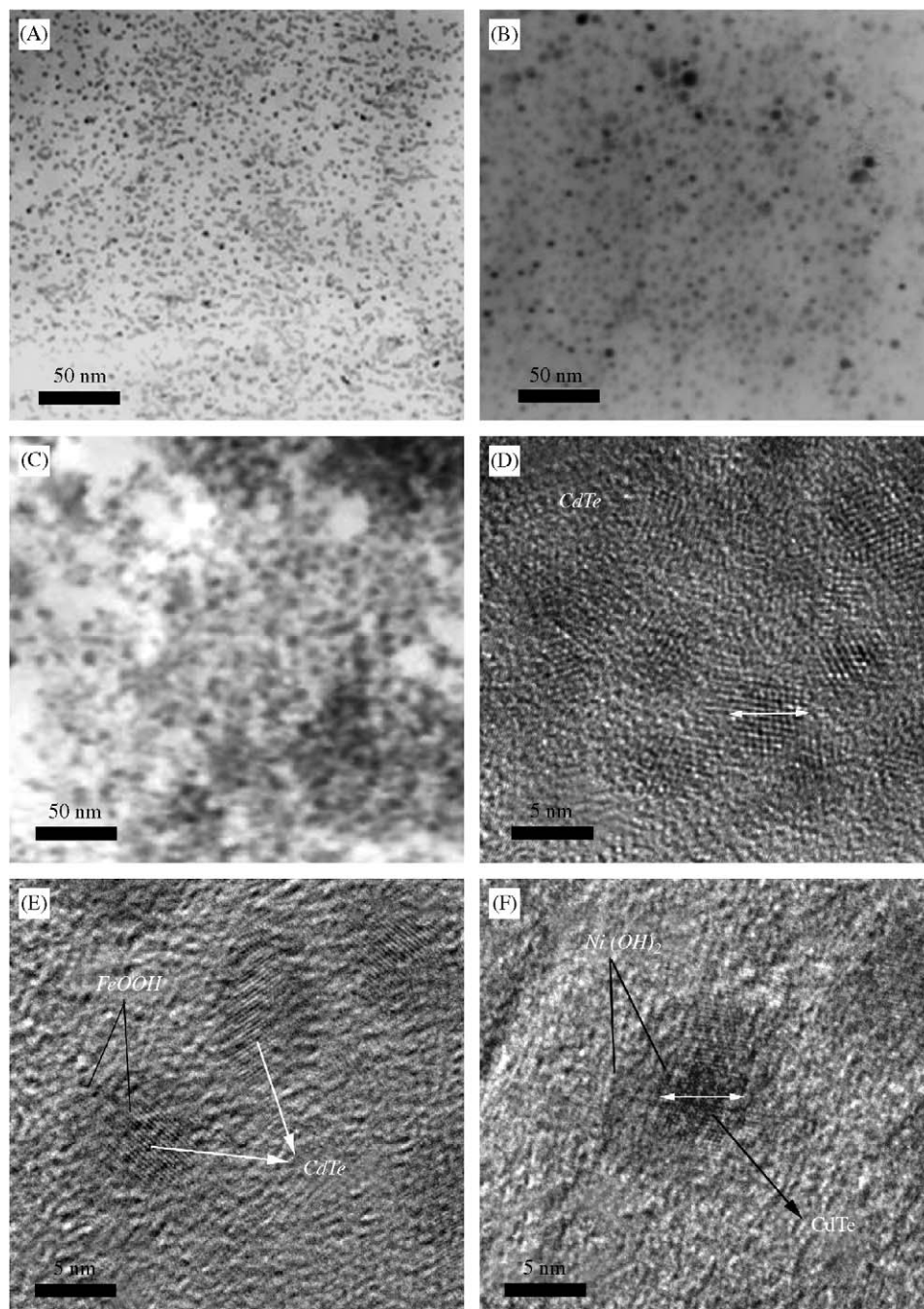


Fig. 3. The TEM images of CdTe NCs (A), CdTe@FeOOH nanoparticles (B) and CdTe@Ni(OH)<sub>2</sub> nanoparticles (C); the HRTEM images of CdTe NCs (D), CdTe@FeOOH nanoparticles (E) and CdTe@Ni(OH)<sub>2</sub> nanoparticles (F).

BE values of 855.9 eV reveals that the Ni mainly exists as Ni(OH)<sub>2</sub>. The weak peak at 854.3 eV indicates that only a very small quantity of NiO presents in the composite nanomaterial [25,26].

Our aim was to obtain two or more functions in an entity particle. The previous reported bi-functional nanomaterials all used magnetic NCs as seeds, whose magnetic properties were dominantly controlled by the magnetic NCs. Here, the magnetic properties of the resulted composite nanomaterials were controlled by the hydroxides on CdTe NCs

surface. The isothermal field-dependent magnetization measured at room temperature is shown in Fig. 6. The results (Figs. 6A and B) indicate the as-prepared CdTe@FeOOH nanoparticles is weak ferromagnetic at 5 K with a coercivity of 193 Oe, but is paramagnetic at 300 K. From the results, we can conclude that its blocking temperature was higher than but near to 5 K, which indirectly indicated the nanoscale nature of the CdTe@FeOOH particles. The magnetization of CdTe@Ni(OH)<sub>2</sub> at 5 K did not show hysteresis behavior, which indicated that the resulted

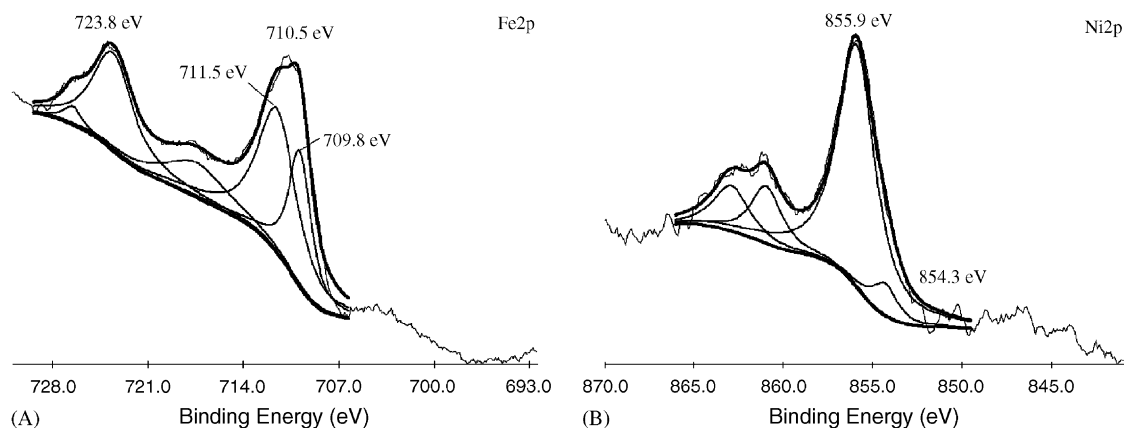


Fig. 4. X-ray photoelectron spectra obtained from the CdTe@FeOOH and CdTe@Ni(OH)<sub>2</sub> nanoparticles recorded at an excitation energy 1253.6 eV. (A) Fe2p; (B) Ni2p.

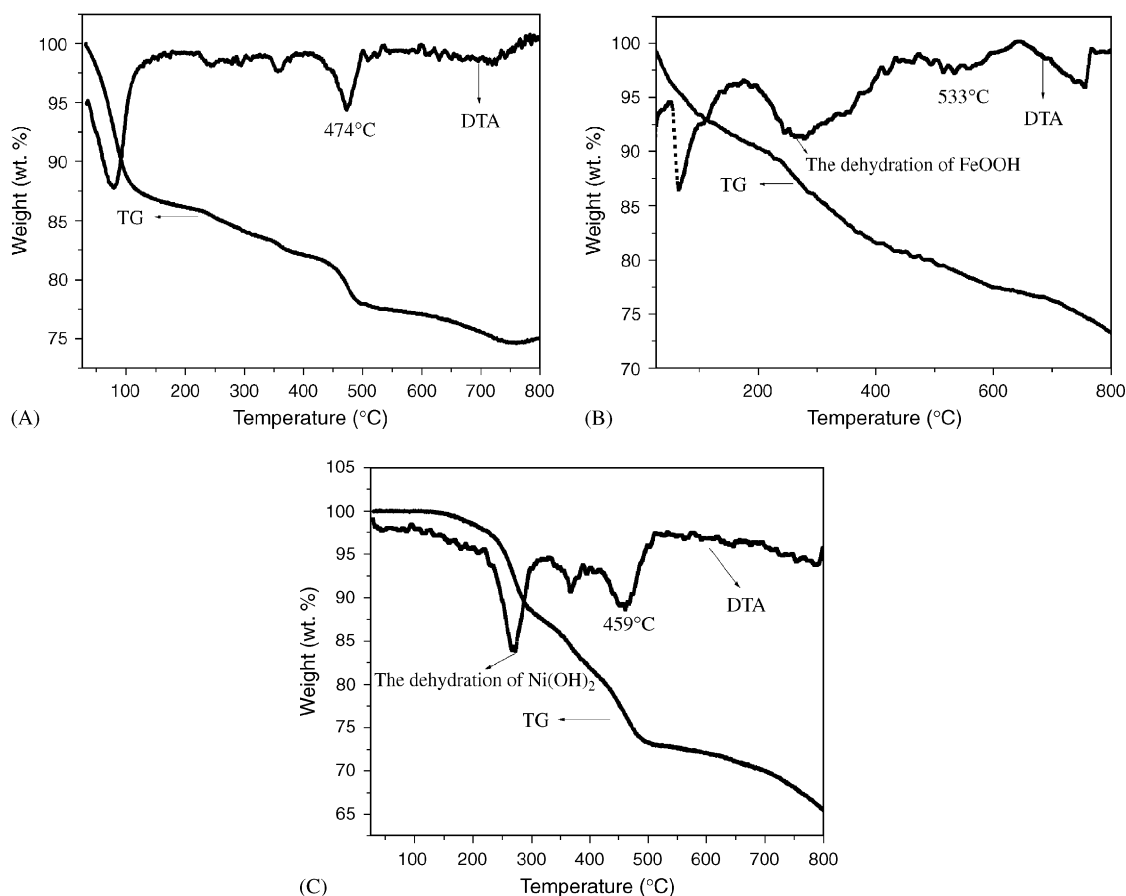


Fig. 5. The DTA and TGA data of bare CdTe NCs (A), CdTe@FeOOH nanoparticles (B) and CdTe@Ni(OH)<sub>2</sub> nanoparticles (C, pre-dried at 110 °C for 5 min under N<sub>2</sub>).

material was superparamagnetic at 5 K, but it lost such a property at 300 K and became a paramagnetic material. It is known that the contrast agents for MR imaging are the chemicals with paramagnetism, which enhances the MR image, including the paramagnetic ions of gadolinium, dysprosium, cobalt, manganese, and iron and combinations thereof [27]. Our composite nanomaterials are not

strong ferromagnetic, but their paramagnetism must be useful in MR imaging.

#### 4. Conclusion

In summary, in this paper we described a method to prepare fluorescent/magnetic composite CdTe@Ni(OH)<sub>2</sub>

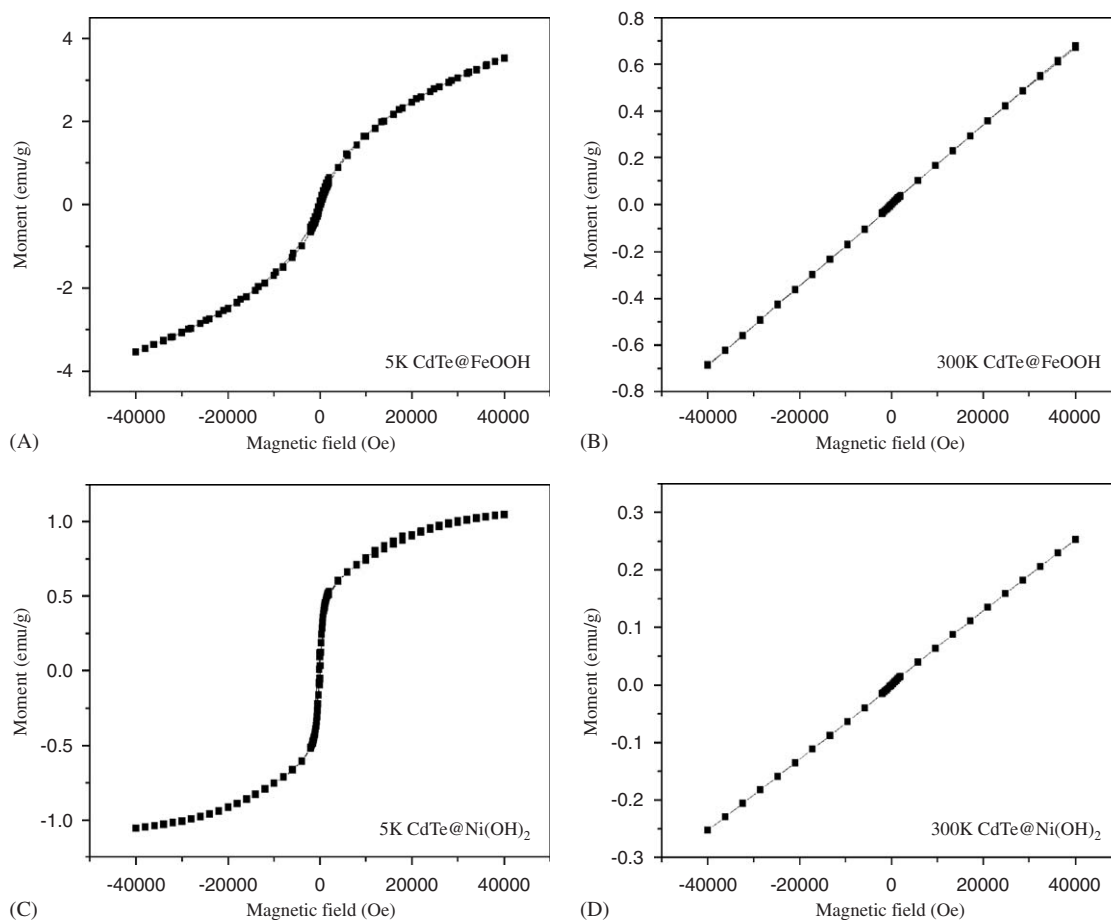


Fig. 6. The field dependence of magnetization for the composite nanoparticles. (A) 5 K, CdTe@FeOOH nanoparticles; (B) 300 K, CdTe@FeOOH nanoparticles; (C) 5 K, CdTe@Ni(OH)<sub>2</sub> nanoparticles; (D) 300 K, CdTe@Ni(OH)<sub>2</sub> nanoparticles.

and CdTe@FeOOH nanoparticles, based on a seed-mediated growth approach. Different from the past reports of fluorescent-magnetic core/shell bi-functional nanomaterials, our approach used the fluorescent NCs as a core, and then deposited a layer of magnetic hydroxides on it. It is known that CdTe NCs presents unique optical and electronic properties, and Fe (Ni) hydroxides possess some important functions (electrochemical activity, magnetism, catalysis). We predict that these multifunctional nanomaterials probably have some potential applications in combined MR/optical imaging, photocatalytic reaction, fabrication of sensors, and energy storage. Furthermore, our synthetic procedure is very simple, mild and cheap, which will be a good choice for synthesis of multifunction nanomaterials.

#### Acknowledgments

This work was financially supported by NSFC (No. 90408014, 20335020, 20571052), the Nano-Science Foundation of Shanghai (0452NM052, 05NM05002).

#### Appendix A. Supplementary data

Supplementary data associated with this article can be found in the online version at [doi:10.1016/j.jssc.2006.03.026](https://doi.org/10.1016/j.jssc.2006.03.026).

#### References

- [1] G. Oldfield, T. Ung, P. Mulvaney, *Adv. Mater.* 12 (2000) 1519.
- [2] L. Wang, J. Luo, M.M. Maye, Q. Fan, Q. Rendeng, M.H. Engelhard, C. Wang, Y. Lin, C.J. Zhong, *J. Mater. Chem.* 15 (2005) 1821.
- [3] A.G. Tkachenko, H. Xie, D. Coleman, W. Glomm, J. Ryan, M.F. Anderson, S. Franzen, D.L. Feldheim, *J. Am. Chem. Soc.* 125 (2003) 4700.
- [4] N. Gaponik, I.L. Radtchenko, G.B. Sukhorukov, A.L. Rogach, *Langmuir* 20 (2004) 1449.
- [5] D. Wang, J. He, N. Rosenzweig, Z. Rosenzweig, *Nano Lett.* 4 (2004) 409.
- [6] H. Gu, R. Zheng, X. Zhang, B. Xu, *J. Am. Chem. Soc.* 126 (2004) 5664.
- [7] H. Kim, M. Achermann, L.P. Balet, J.A. Hollingsworth, V.I. Klimov, *J. Am. Chem. Soc.* 127 (2005) 544.
- [8] D.K. Yi, S.T. Selvan, S.S. Lee, G.C. Papaefthymiou, D. Kundaliya, J.Y. Ying, *J. Am. Chem. Soc.* 127 (2005) 4990.
- [9] H. Yu, M. Chen, P.M. Rice, S.X. Wang, R.L. White, S. Sun, *Nano Lett.* 5 (2005) 379.

- [10] L. Li, H. Qian, J.C. Ren, *Chem. Commun.* 32 (2005) 4083.
- [11] L. Li, H. Qian, N.H. Fang, J.C. Ren, *J. Lumin.* 116 (2006) 59.
- [12] L. Li, H. Qian, J.C. Ren, *Chem. Commun.* 4 (2005) 528.
- [13] H. Liu, Y. Wei, Y.H. Sun, W. Wei, *Colloids Surf. A: Physicochem. Eng. Aspects* 252 (2005) 201.
- [14] M. Ristić, S. Musić, M. Godec, *J. Alloys Compd.* (2005).
- [15] G.A. Crosby, J.N. Demas, *J. Phys. Chem.* 75 (1971) 991.
- [16] D.H. Son, S.M. Hughes, Y. Yin, A.P. Alivisatos, *Science* 306 (2004) 1009.
- [17] Y.X. Han, X.S. Ma, H.M. Cao, H.Y. Zhang, Q.F. Wu, *Mater. Res. Bull.* 39 (2004) 1159.
- [18] I. Mitov, D. Paneva, B. Kunev, *Thermochim. Acta* 386 (2002) 179.
- [19] H.B. Zhang, H.S. Liu, X.J. Cao, S.J. Li, C.C. Sun, *Mater. Chem. Phys.* 79 (2003) 37.
- [20] X.M. He, J.J. Li, H.W. Cheng, C.Y. Jiang, C.R. Wan, *J. Power Sources* 152 (2005) 285.
- [21] G.T. Zhou, Q.Z. Yao, X.C. Wang, J.C. Yu, *Mater. Chem. Phys.* (2005).
- [22] NIST Standard Reference Database 20, Version 3.4.
- [23] N.S. McIntyre, D.G. Zetaruk, *Anal. Chem.* 49 (1977) 1521.
- [24] N. Ruiz, S. Seal, D. Reinhart, *J. Hazard. Mater. B* 80 (107–117) (2000) 6.
- [25] N. Hernandez, R. Moreno, A.J. Sanchez-Herencia, J.L.G. Fierro, *J. Phys. Chem. B* 109 (2005) 4470.
- [26] T. Yoshida, T. Tanaka, H. Yoshida, T. Funabiki, S. Yoshida, *J. Phys. Chem.* 100 (1996) 2302.
- [27] M.W. Brechbiel, R.A. Star, H. Kobayashi, United States Patent No: 6852842.